

# Fluidistic description of astrophysical and space plasmas

## - Part 2 -

*Daniel Gómez<sup>1,2</sup>*



(1) Departamento de Física, Fac. Cs. Exactas y Naturales, UBA, Argentina

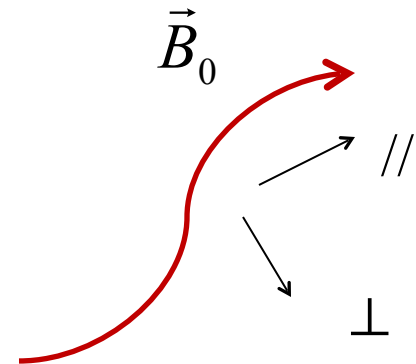
(2) Instituto de Astronomía y Física del Espacio, UBA-CONICET, Argentina

# Two-fluid MHD

- ➡ MHD is a fluidistic approach to describe the large scale dynamics of plasmas.
- ➡ The standard approach is also known as one-fluid MHD.
- ➡ We are going to start from a somewhat more general approach known as two-fluid MHD, which acknowledges the presence of ions and electrons and considers kinetic effects such as Hall, electron pressure and electron inertia.

➡ Physical processes that can be addressed with MHD include:

- Magnetic reconnection
- Magnetic confinement
- Magnetic dynamo
- MHD shocks
- MHD turbulence



- ➡ We will also address the case of plasmas embedded in strong external magnetic fields, which allow for an approximation known as reduced MHD, both for one-fluid MHD (RMHD) and two-fluid MHD (RHMHD).

# Fluid equations for multi-species plasmas

➡ For each species  $s$  we have (Goldston & Rutherford 1995):

▶ Mass conservation 
$$\frac{\partial n_s}{\partial t} + \vec{\nabla} \cdot (n_s \vec{U}_s) = 0$$

▶ Equation of motion 
$$m_s n_s \frac{d\vec{U}_s}{dt} = q_s n_s (\vec{E} + \frac{1}{c} \vec{U}_s \times \vec{B}) - \vec{\nabla} p_s + \vec{\nabla} \cdot \vec{\sigma}_s + \sum_{s'} \vec{R}_{ss'}$$

▶ Momentum exchange rate 
$$\vec{R}_{ss'} = -m_s n_s \nu_{ss'} (\vec{U}_s - \vec{U}_{s'})$$

➡ These moving charges act as sources for electric and magnetic fields:

▶ Charge density 
$$\rho_c = \sum_s q_s n_s \approx 0$$

▶ Electric current density 
$$\vec{J} = \frac{c}{4\pi} \vec{\nabla} \times \vec{B} = \sum_s q_s n_s \vec{U}_s$$

# Small scales: EIH MHD equations

→ The dimensionless version, for a length scale  $L_0$ , density  $n_0$  and Alfvén speed  $v_A = B_0 / \sqrt{4\pi m_i n_0}$

$$\frac{d\vec{U}_i}{dt} = \frac{1}{\varepsilon} (\vec{E} + \vec{U}_i \times \vec{B}) - \frac{\beta}{n} \vec{\nabla} p_i - \frac{\eta}{\varepsilon n} \vec{J}$$

$$\frac{m_e}{m_i} \frac{d\vec{U}_e}{dt} = -\frac{1}{\varepsilon} (\vec{E} + \vec{U}_e \times \vec{B}) - \frac{\beta}{n} \vec{\nabla} p_e + \frac{\eta}{\varepsilon n} \vec{J} \quad \text{where} \quad \vec{J} = \vec{\nabla} \times \vec{B} = \frac{n}{\varepsilon} (\vec{U}_i - \vec{U}_e)$$

→ We define the Hall parameter  $\varepsilon = \frac{c}{\omega_{pi} L_0}$

as well as the plasma beta  $\beta = \frac{p_0}{m_i n_0 v_A^2}$  and the electric resistivity  $\eta = \frac{c^2 \nu_{ie}}{\omega_{pi}^2 L_0 v_A}$

→ Adding these two equations yields:

$$\frac{d\vec{U}}{dt} = (\vec{\nabla} \times \vec{B}) \times (\vec{B} + \varepsilon_e^2 \vec{\nabla} \times \vec{J}) - \vec{\nabla} p$$

where  $\vec{U} = \frac{m_i \vec{U}_i + m_e \vec{U}_e}{m_i + m_e}$

and  $p = p_i + p_e$

$$\varepsilon_e = \sqrt{\frac{m_e}{m_i}} \varepsilon = \frac{c}{\omega_{pe} L_0}$$

# Ideal invariants in EIH MHD

→ For each species  $s$  in the incompressible and ideal limit

$$m_s n_s \left( \partial_t \vec{U}_s - \vec{U}_s \times \vec{W}_s \right) = q_s n_s \left( \vec{E} + \frac{1}{c} \vec{U}_s \times \vec{B} \right) - \vec{\nabla} \left( p_s + m_s n_s \frac{U_s^2}{2} \right)$$

→ Using that  $\vec{J} = \frac{c}{4\pi} \vec{\nabla} \times \vec{B} = \sum_s q_s n_s \vec{U}_s$  and  $E = -\frac{1}{c} \partial_t \vec{A} - \vec{\nabla} \phi$

we can readily show that energy is an ideal invariant, where

$$E = \int d^3 r \left( \sum_s m_s n_s \frac{U_s^2}{2} + \frac{B^2}{8\pi} \right)$$

→ We also have a helicity per species which is conserved, where

$$H_s = \int d^3 r \left( \vec{A} + \frac{cm_s}{q_s} \vec{U}_s \right) \cdot \left( \vec{B} + \frac{cm_s}{q_s} \vec{W}_s \right)$$

# Normal modes in EIH MHD

- ➔ If we linearize our equations around an equilibrium characterized by a uniform magnetic field, we obtain the following dispersion relation:

$$\left( \frac{\omega}{\vec{k} \cdot \vec{B}_0} \right)^2 \pm \frac{k\epsilon}{1 + \epsilon_e^2 k^2} \left( \frac{\omega}{\vec{k} \cdot \vec{B}_0} \right) - \frac{1}{1 + \epsilon_e^2 k^2} = 0$$

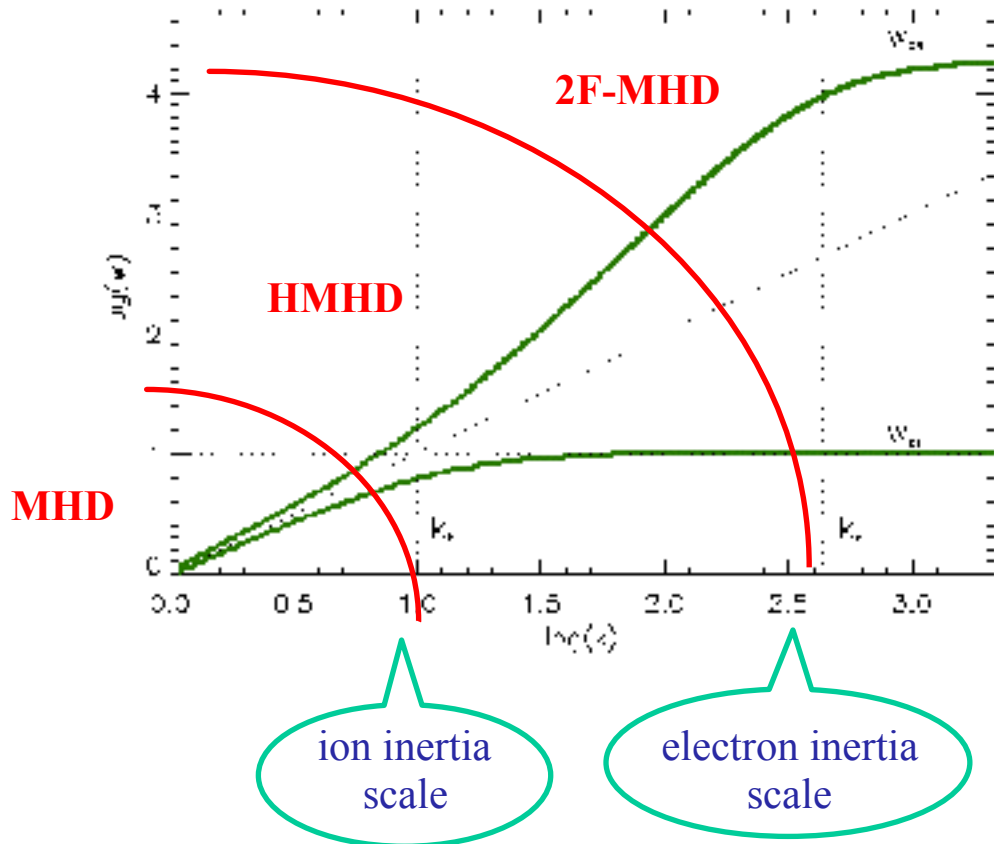
- ➔ Asymptotically, at very large  $k$ , we have two branches

$$\omega \xrightarrow{k \rightarrow \infty} \omega_{ce} \cos \theta$$

$$\omega \xrightarrow{k \rightarrow \infty} \omega_{ci} \cos \theta$$

while for very small  $k$ , both branches simply become Alfvén modes, i.e.

$$\omega \xrightarrow{k \rightarrow 0} k \cos \theta$$



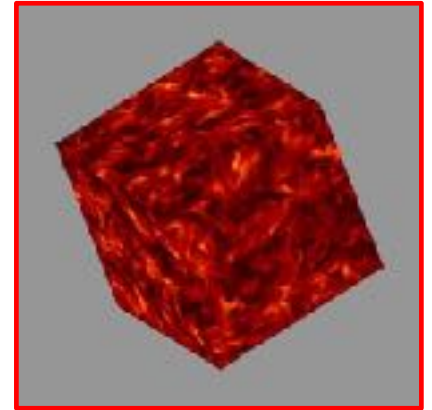
- ➔ Different approximations, just as one-fluid MHD, Hall-MHD and electron-inertia MHD can clearly be identified in this diagram.

# Some applications

## MHD

RMHD heating of solar coronal loops ([Dmitruk & Gomez 1997, 1999](#))

Kelvin-Helmholtz instability in the solar corona ([Gomez, DeLuca & Mininni 2016](#))



## HALL-MHD

3D HMHD turbulent dynamos. ([Mininni, Gomez & Mahajan 2003, 2005](#); [Gomez, Dmitruk & Mininni 2010](#))

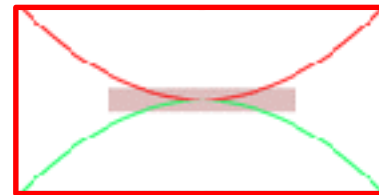
2.5 D HMHD reconnection at Earth magnetopause ([Morales, Dasso & Gomez 2005, 2006](#))

RHMHD turbulence in the solar wind ([Martin, Dmitruk & Gomez 2010, 2012](#))

Hall MRI in accretion disks ([Bejarano, Gomez & Brandenburg 2011](#))

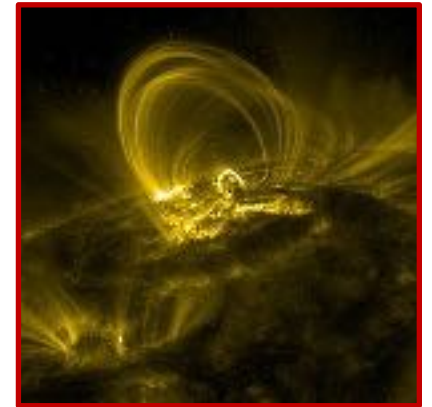
## Electron inertia

1D model of perpendicular shocks ([Gomez et al. 2018](#)).



Two-fluid turbulence in the solar wind ([Andres et al. 2014, 2016](#)).

Fast reconnection in 2.5 D ([Andres, Dmitruk & Gomez 2014, 2016](#)).



# HALL-MHD equations

→ The dimensionless version, for a length scale  $L_0$ , density  $n_0$  and Alfven speed

$$v_A = B_0 / \sqrt{4\pi m_i n_0}$$

$$\frac{d\vec{U}}{dt} = \frac{1}{\varepsilon} (\vec{E} + \vec{U} \times \vec{B}) - \frac{\beta}{n} \vec{\nabla} p_i - \frac{\eta}{\varepsilon n} \vec{J} + \nu \nabla^2 \vec{U}$$

$$\nu = \frac{\mu}{m_i n v_A L_0}$$

$$0 = -\frac{1}{\varepsilon} (\vec{E} + \vec{U}_e \times \vec{B}) - \frac{\beta}{n} \vec{\nabla} p_e + \frac{\eta}{\varepsilon n} \vec{J} \quad \text{where} \quad \vec{J} = \vec{\nabla} \times \vec{B} = \frac{n}{\varepsilon} (\vec{U} - \vec{U}_e)$$

→ We define the Hall parameter  $\varepsilon = \frac{c}{\omega_{pi} L_0}$

as well as the plasma *beta*  $\beta = \frac{p_0}{m_i n_0 v_A^2}$  and the electric resistivity  $\eta = \frac{c^2 \nu_{ie}}{\omega_{pi}^2 L_0 v_A}$

→ Adding these two equations yields:

$$n \frac{d\vec{U}}{dt} = (\vec{\nabla} \times \vec{B}) \times \vec{B} - \beta \vec{\nabla} (p_i + p_e) + \nu \nabla^2 \vec{U}$$

→ On the other hand, using

$$\left. \begin{aligned} \vec{E} &= -\frac{1}{c} \frac{\partial \vec{A}}{\partial t} - \vec{\nabla} \phi \\ \vec{B} &= \vec{\nabla} \times \vec{A} \end{aligned} \right\}$$

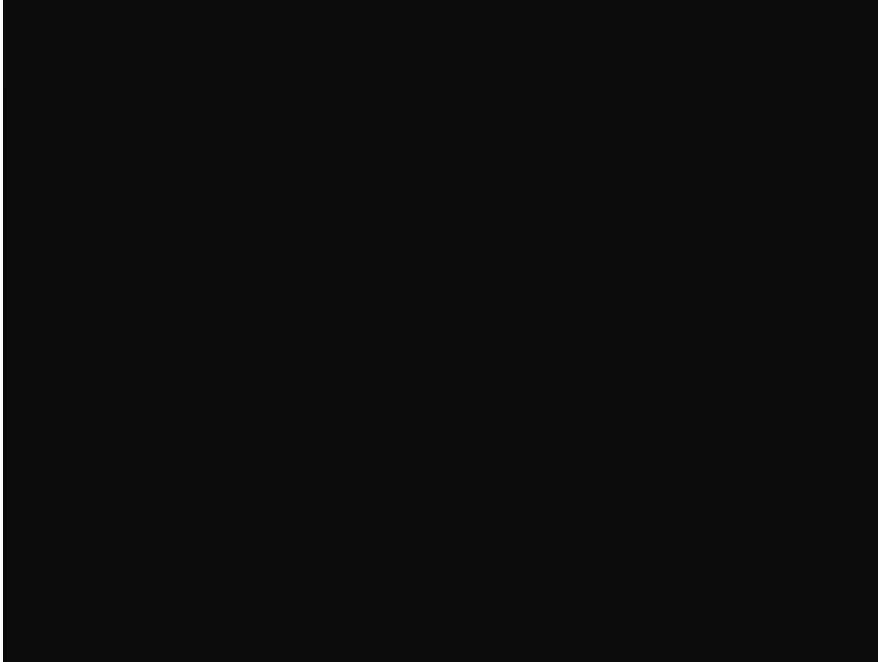


$$\frac{\partial \vec{A}}{\partial t} = (\vec{U} - \frac{\varepsilon}{n} \vec{\nabla} \times \vec{B}) \times \vec{B} - \vec{\nabla} \phi + \frac{\varepsilon \beta}{n} \vec{\nabla} p_e - \frac{\eta}{n} \vec{\nabla} \times \vec{B}$$

Hall-MHD  
equations



# RMHD applied to coronal loop heating



- ➡ The solar corona is a topologically complex array of loops (TRACE movie 171 A)
- ➡ Coronal loops are magnetic flux tubes with their footpoints anchored deep in the convective region.
- ➡ They confine a tenuous and hot plasma. Typical densities are  $n = 10^9 \text{ cm}^{-3}$  and temperatures are  $T = 2\text{-}3 \cdot 10^6 \text{ K}$ .
- ➡ The magnetic field provides not just the confinement of the plasma, but also the energy to heat it up to coronal temperatures (Parker 1972, 1988; van Ballegooijen 1986; Einaudi et al. 1996).
- ➡ One of the key ingredients is the free energy available in the sub-photospheric convective region. Convective motions move the footpoints of fieldlines, thus building up magnetic stresses. See Mandrini, Demoulin & Klimchuk 2000 for a comprehensive comparison between theoretical models and observations for a large number of active regions.
- ➡ However, the typical length scale of these magnetic stresses is way too large for the Ohmic dissipation to do the job, since

$$\tau_{diss} \approx \ell^2 / \eta$$

# RMHD Equations

- ➔ Reduced MHD is a self-consistent approximation of the full MHD equations whenever:
- (a) one component of the magnetic field is much stronger than the others and,
  - (b) spatial variations are smoother along than across (Strauss 1976).

$$\partial_t a = v_A \partial_z \varphi + [\varphi, a] + \eta \nabla_\perp^2 a$$

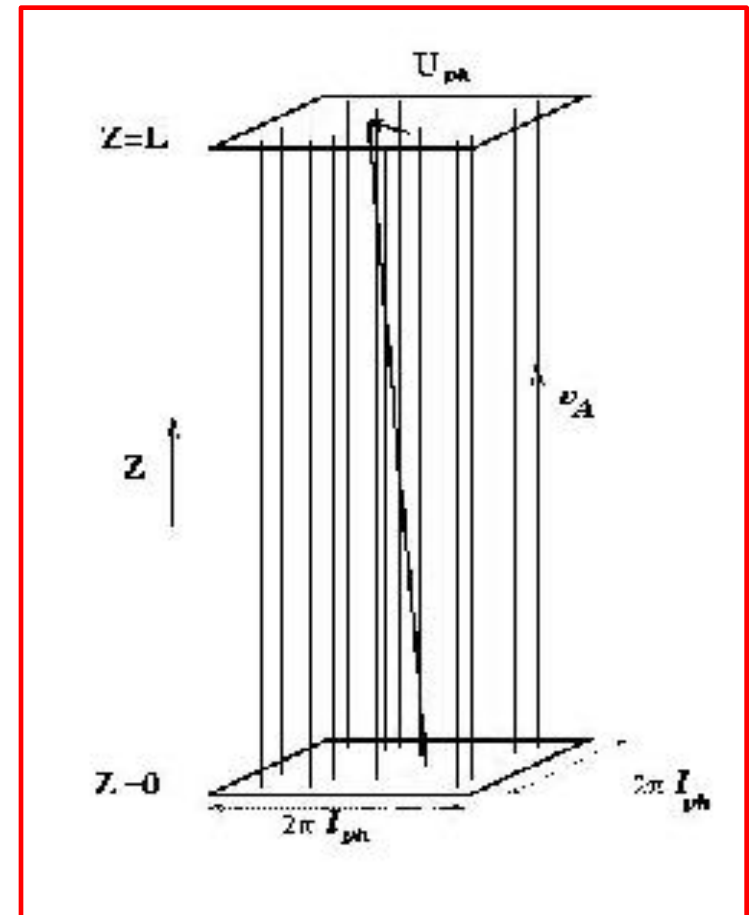
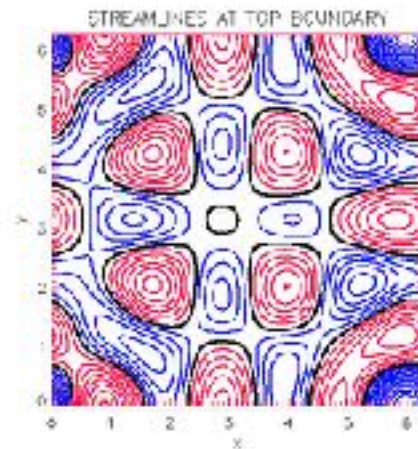
$$\partial_t \omega = v_A \partial_z j + [\varphi, \omega] - [a, j] + \eta \nabla_\perp^2 \omega$$

$$\vec{b} = v_A \hat{z} + \vec{\nabla}_\perp \times (a \hat{z}) \quad , \quad \vec{u} = \vec{\nabla}_\perp \times (\varphi \hat{z})$$

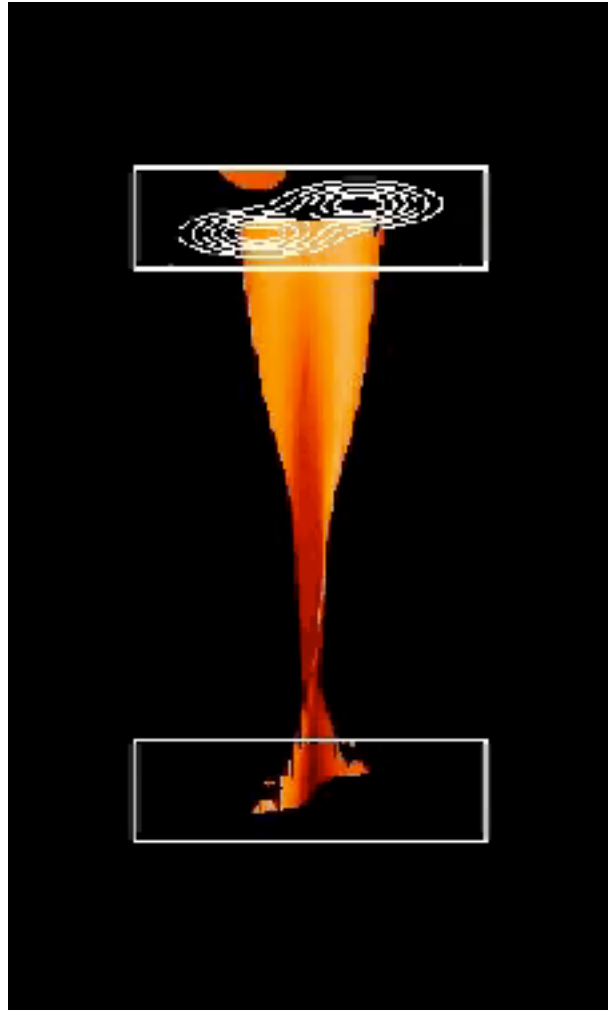
$$\omega = -\nabla_\perp^2 \varphi \quad , \quad j = -\nabla_\perp^2 a$$

- ➔ These equations describe the evolution of the velocity (u) and magnetic field (b) inside the box, assuming periodic boundary conditions at the sides.

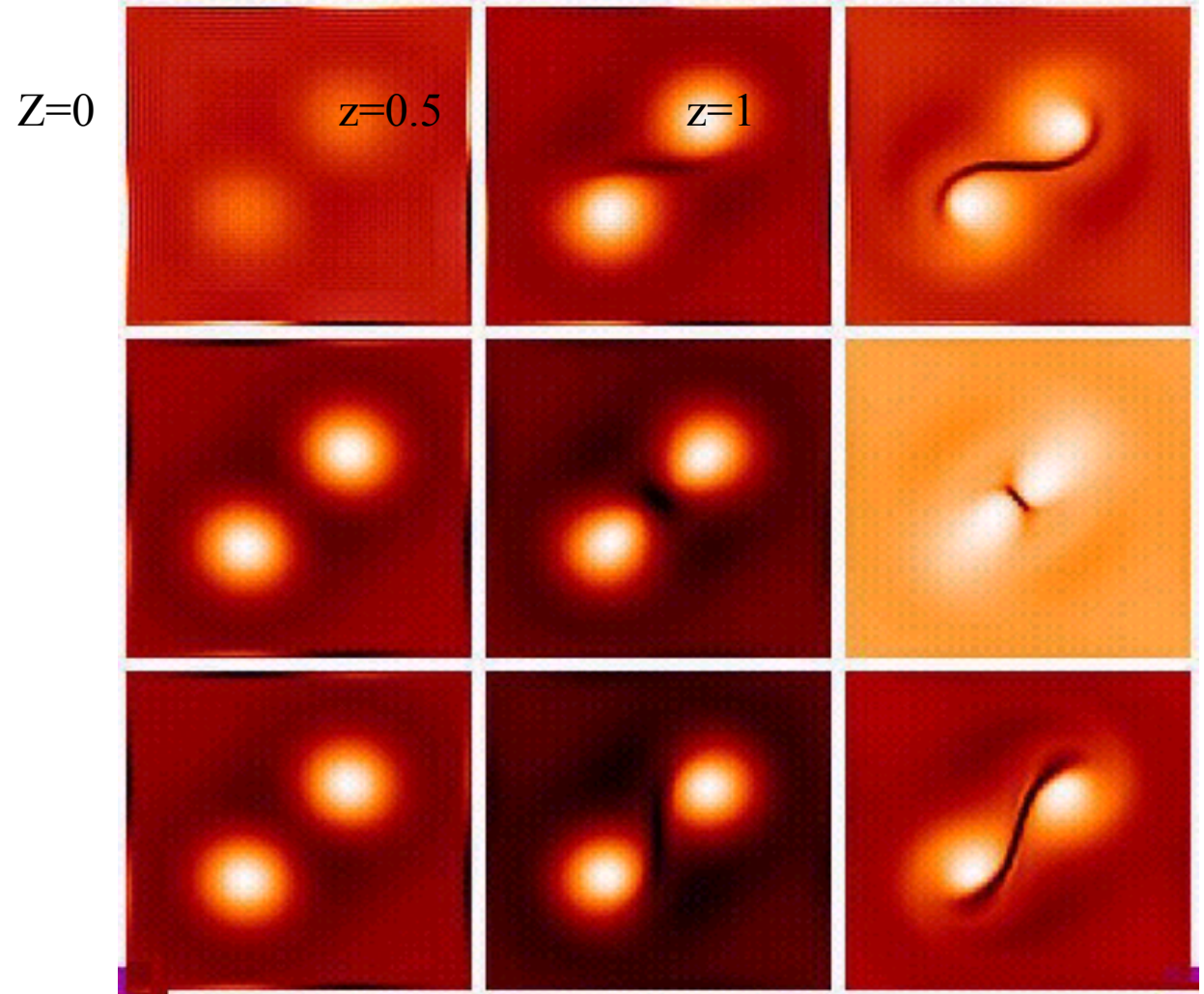
- ➔ We enforce stationary velocity field ( $U_{ph}$ ) at the top plate.



# Current density distribution



Current density

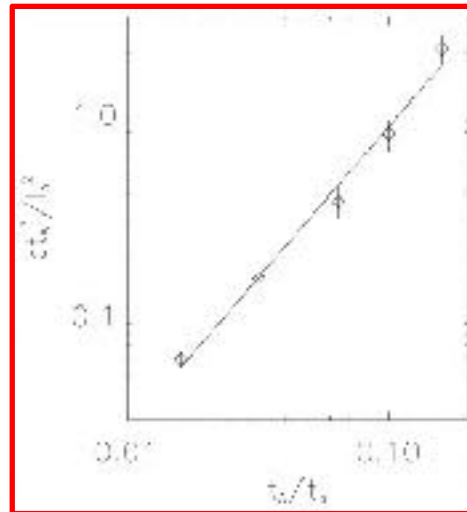


time  $\longrightarrow$

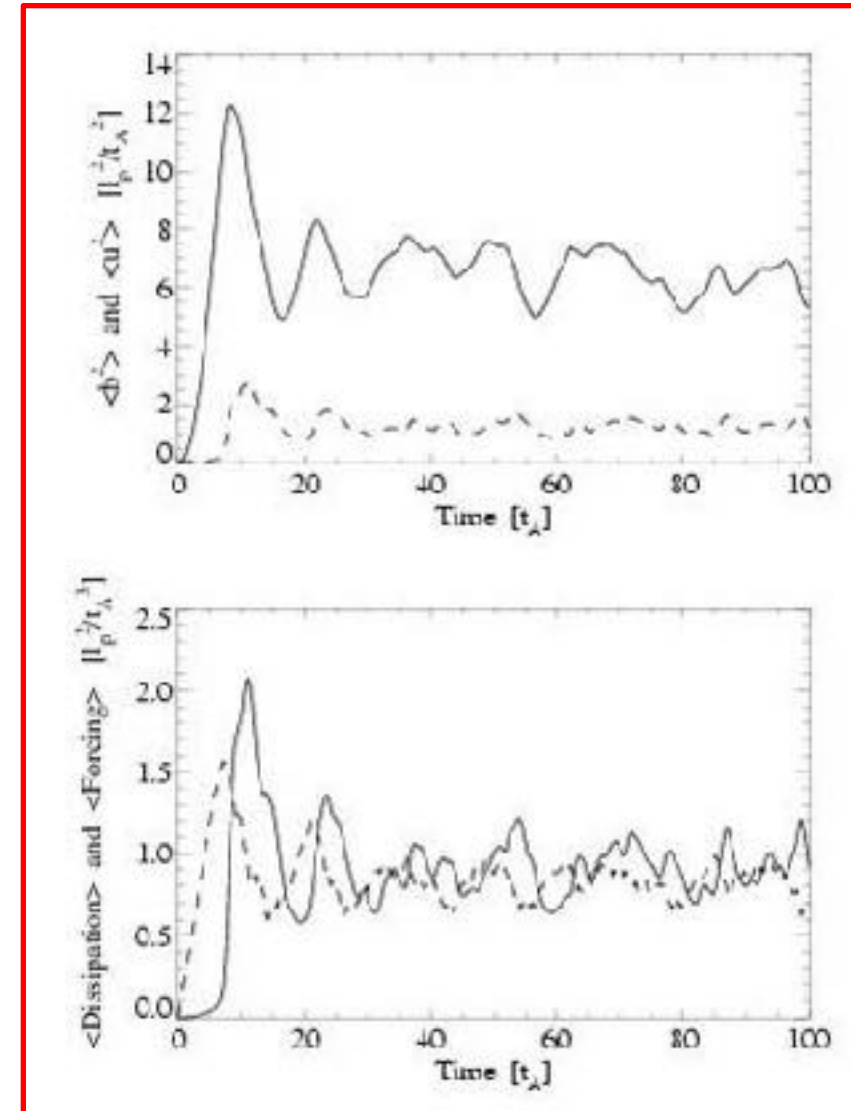
# RMHD simulations

- ➡ We perform long time integrations of the RMHD equations. Lengths are in units of the photospheric motions ( $\ell_{ph}$ ) and times are in units of the Alfvén time ( $t_A$ ) along the loop.
- ➡ Spatial resolution is  $256 \times 256 \times 48$  and the integration time is  $4000 t_A$ . We use a spectral scheme in the xy-plane and finite differences along z.
- ➡ The time averaged dissipation rate is found to scale like (Dmitruk & Gómez 1999)

$$\varepsilon \approx \frac{\rho \ell_{ph}^2}{t_A^3} \left( \frac{t_A}{t_{ph}} \right)^{3/2}$$



- ➡ It is essentially independent of the Reynolds number, as expected for stationary turbulence.



# Stationary turbulence

## → Energy cascade

- energy flux toward high  $k$
- vortex breakdown

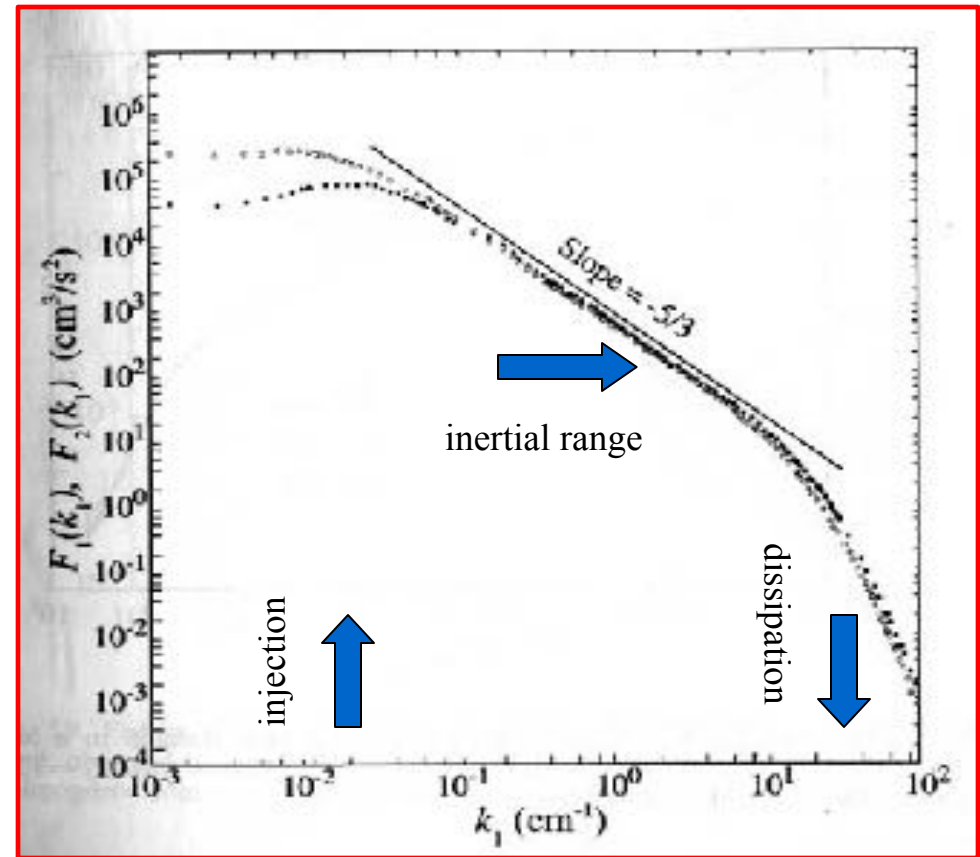
## → Scale invariance

- energy flux in  $k$ :  $\rightarrow \epsilon_k \approx \frac{u_k^2}{\tau_k}$
- energy power spectrum:  $\rightarrow E_k \approx \frac{u_k^2}{k}$

$$\tau_k \approx \frac{1}{ku_k}, \quad \epsilon_k \approx \frac{u_k^2}{\tau_k} = \text{const.}$$

## → Therefore

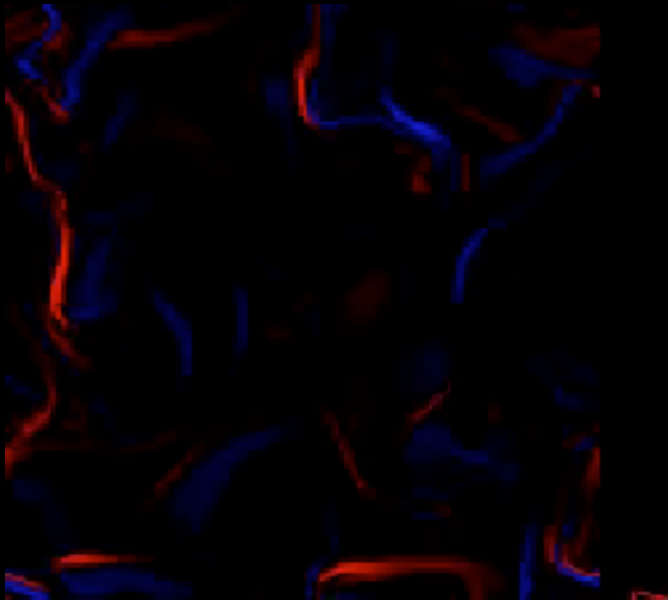
$$E_k \approx \frac{u_k^2}{k} = \epsilon \frac{2}{3} k^{-\frac{5}{3}}$$



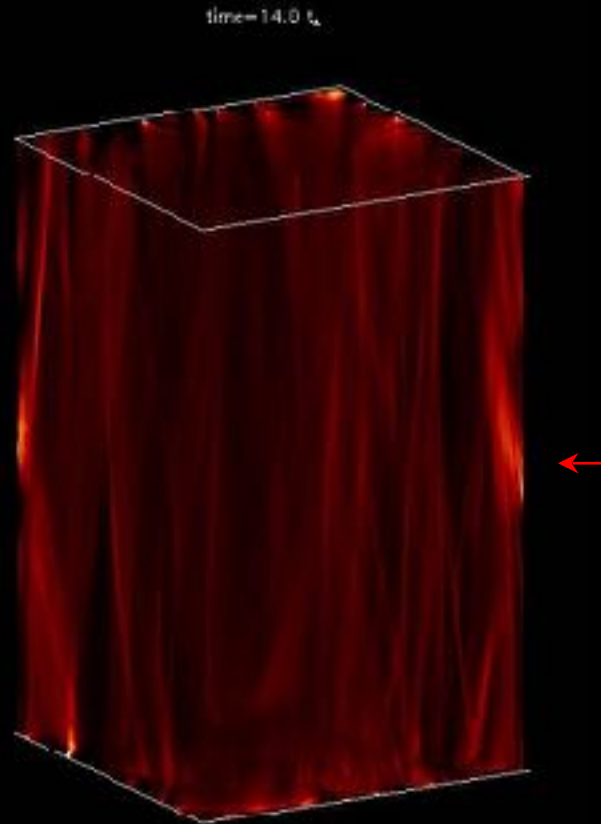
Kolmogorov spectrum (K41)

# Dissipative structures: current sheets in 2D

Most of the energy dissipation takes place in current sheets. We display the current density (upflows & downflows) along the loop in a transverse cut.



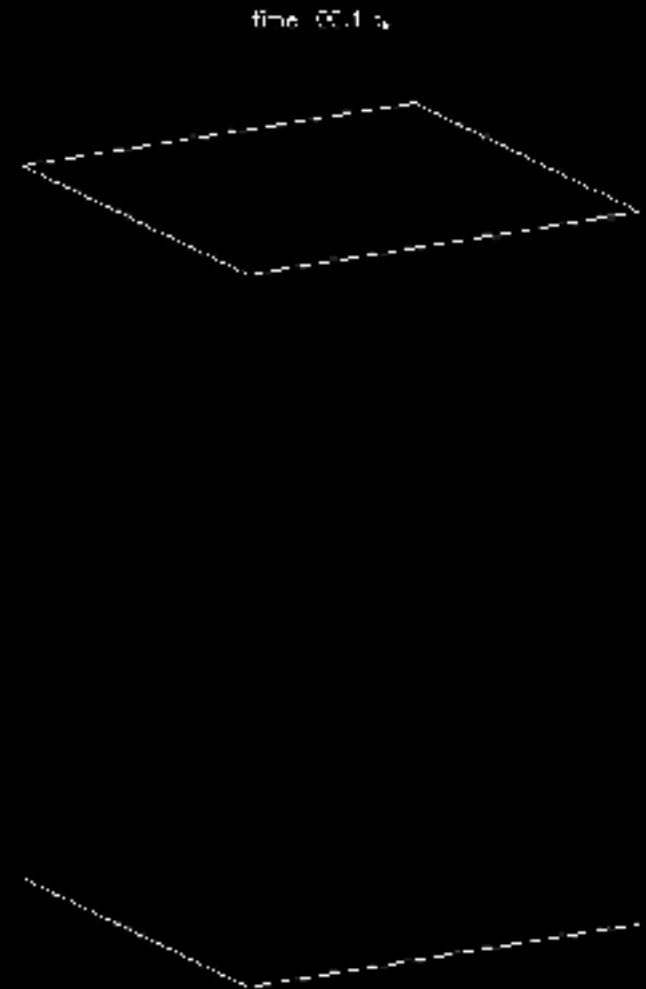
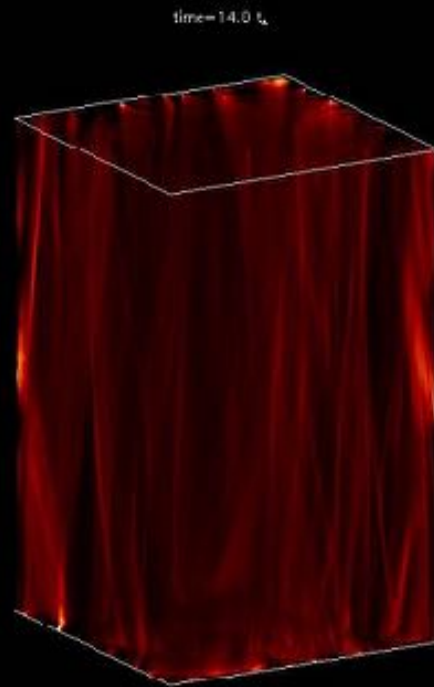
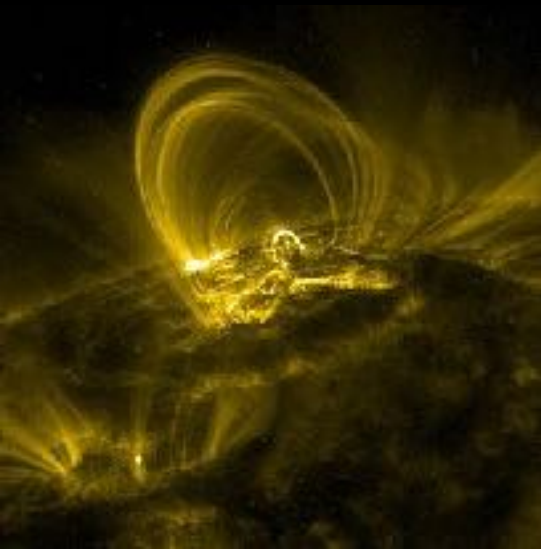
Versus height.



Versus time.

# Dissipative structures: current sheets in 3D

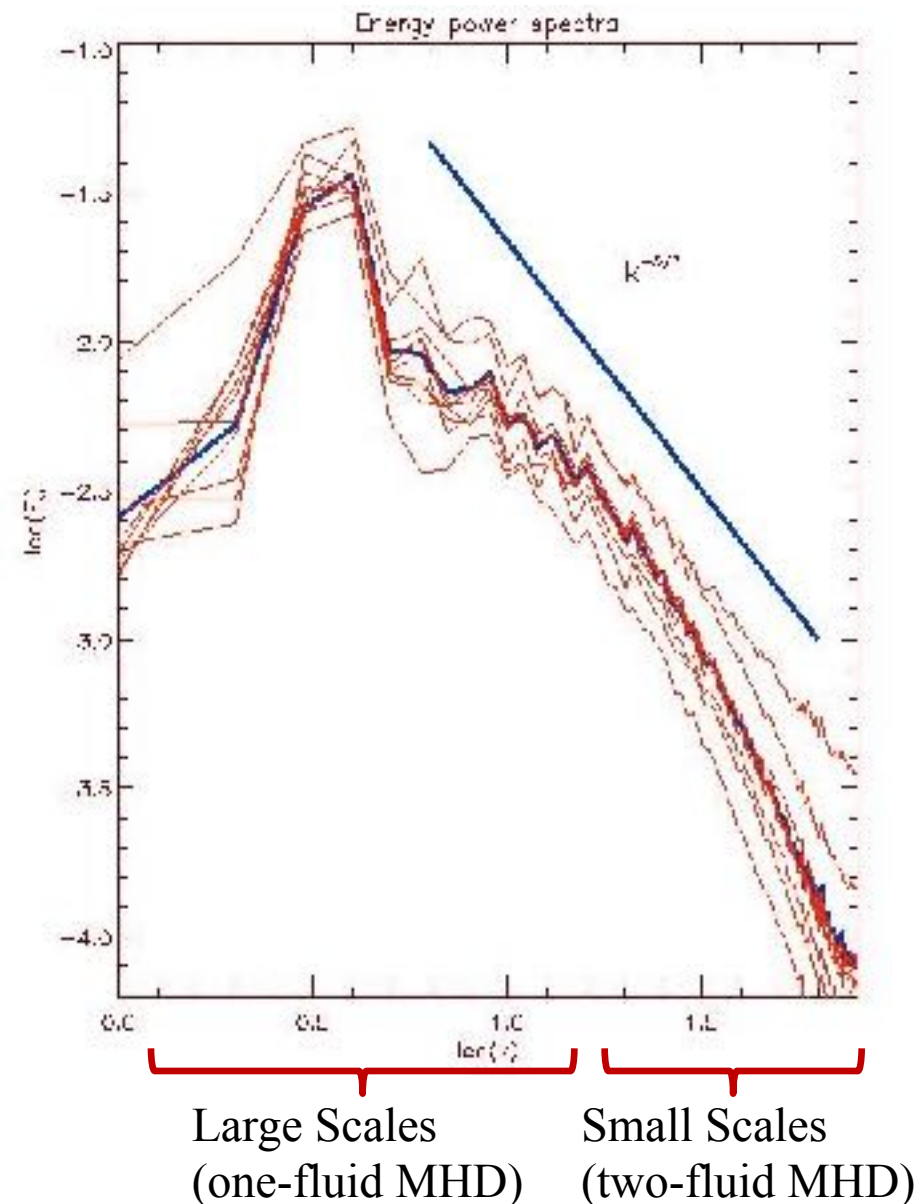
- 3D distribution of the energy dissipation rate.
- We display the dissipation rate during 20 Alfvén times with a cadence of  $0.1 t_A$ .





# Large and small scales: Energy power spectra

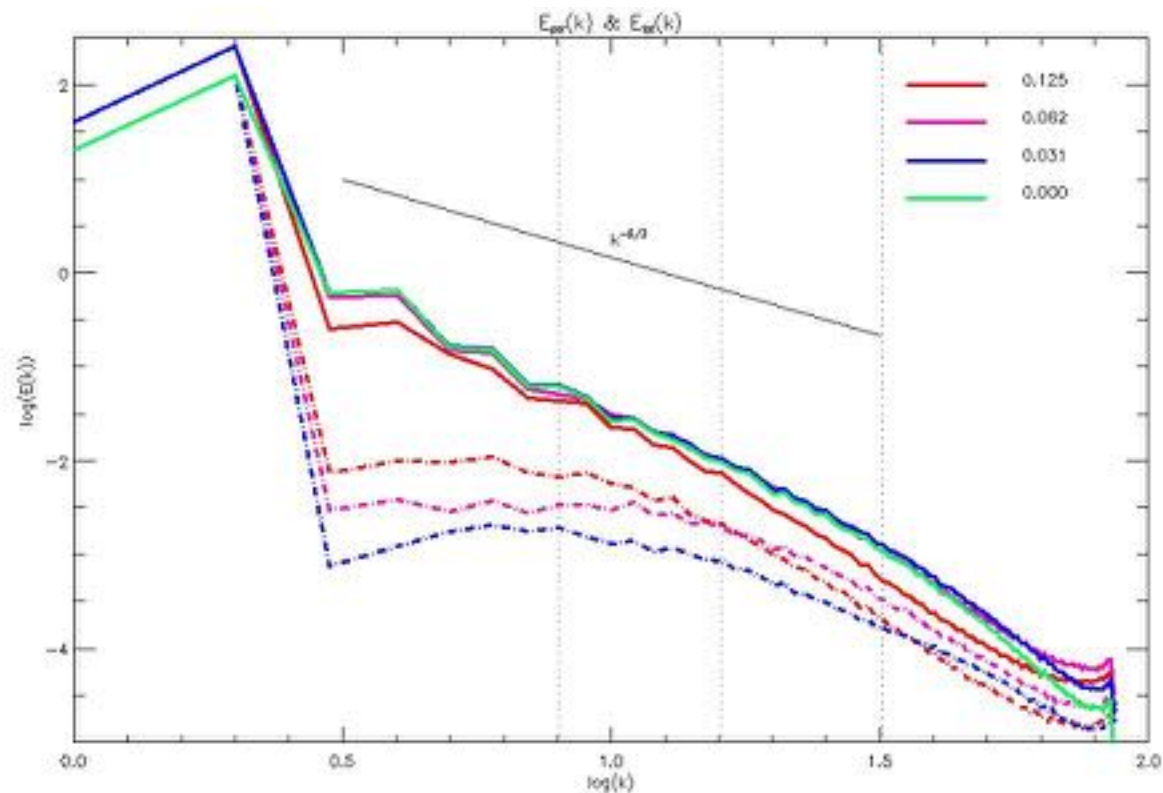
- ➡ The energy spectra are shown here. The **red lines** correspond to ten spectra taken at different times (separated by  $10 t_A$ ). The **blue trace** is the time averaged version.
- ➡ The Kolmogorov slope is displayed for reference, but the moderate spatial resolution of these runs is insufficient for a serious spectral analysis.
- ➡ Viscosity and resistivity are large enough to spatially resolve the dissipative structures properly.
- ➡ In one-fluid MHD, the only kinetic effects were viscosity and resistivity. A two-fluid description would bring new physics into play.





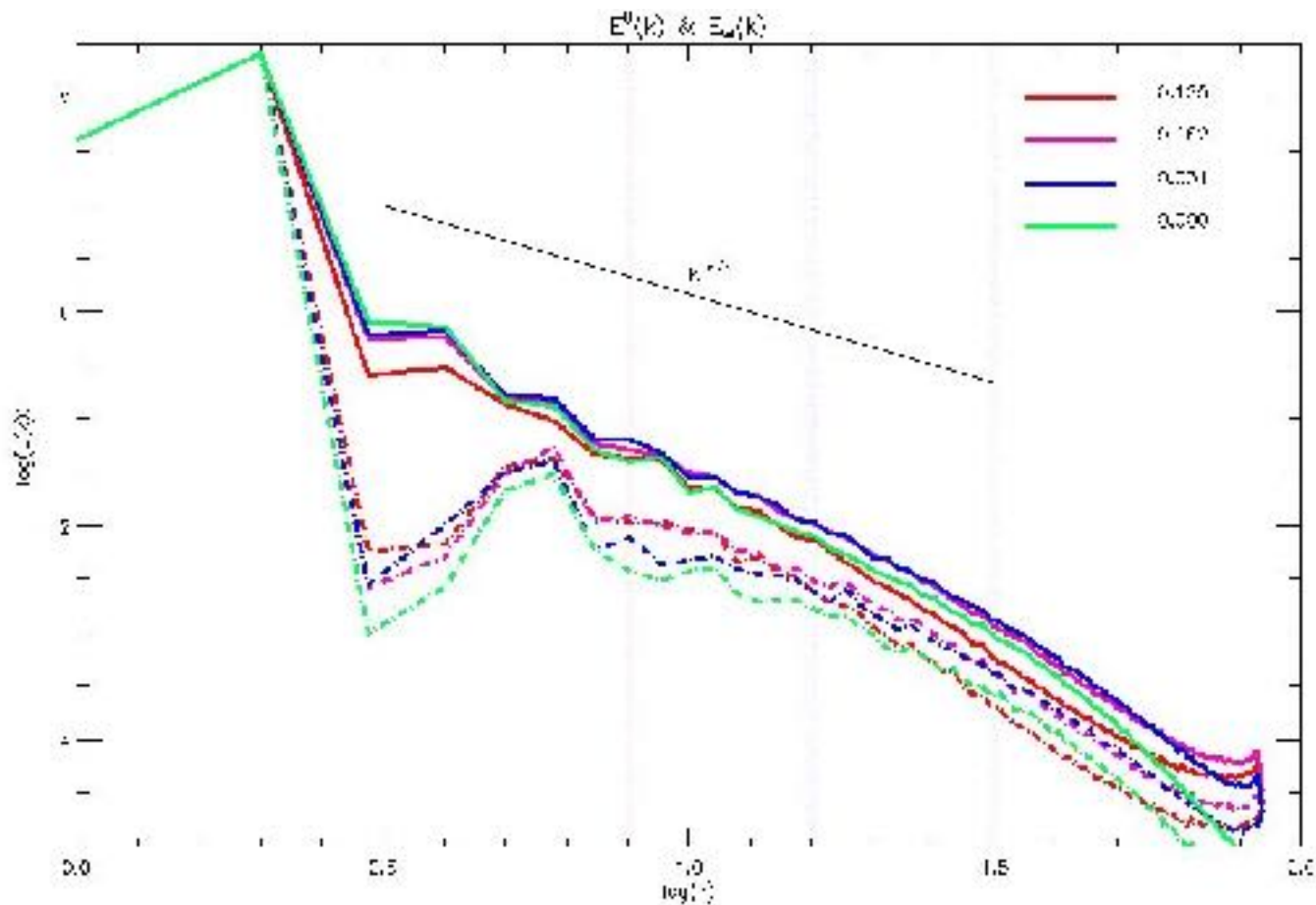
# Energy spectra

- ➔ We also computed energy power spectra for different values of the Hall parameter  $\varepsilon$ .
- ➔ The Kolmogorov slope  $k^{-5/3}$  is also displayed for reference.
- ➔ The dotted curves correspond to the parallel energy spectra.
- ➔ The vertical dotted lines indicate the location of the Hall scale  $k_\varepsilon \cong 1/\varepsilon$  for each run.



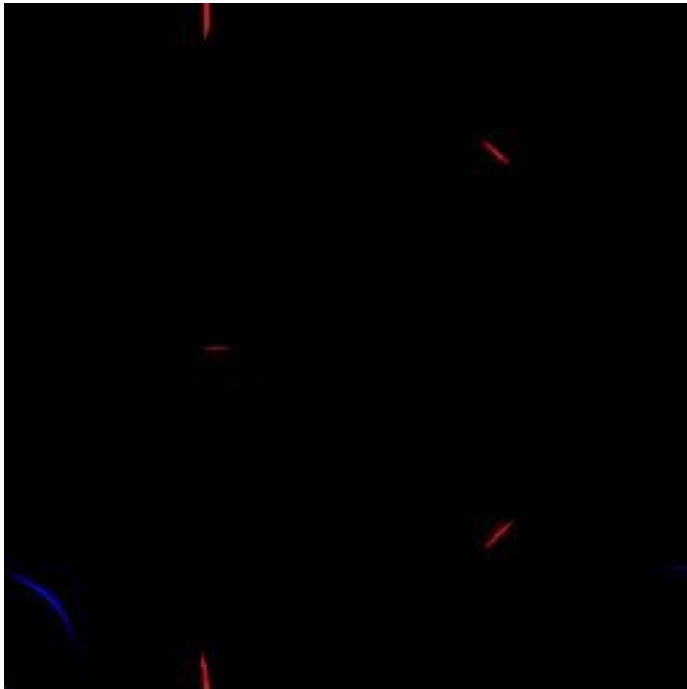
# Energy spectra

- ➔ Energy power spectra for different values of  $\varepsilon$ .
- ➔ The dotted curves are the spectra for kinetic energy.

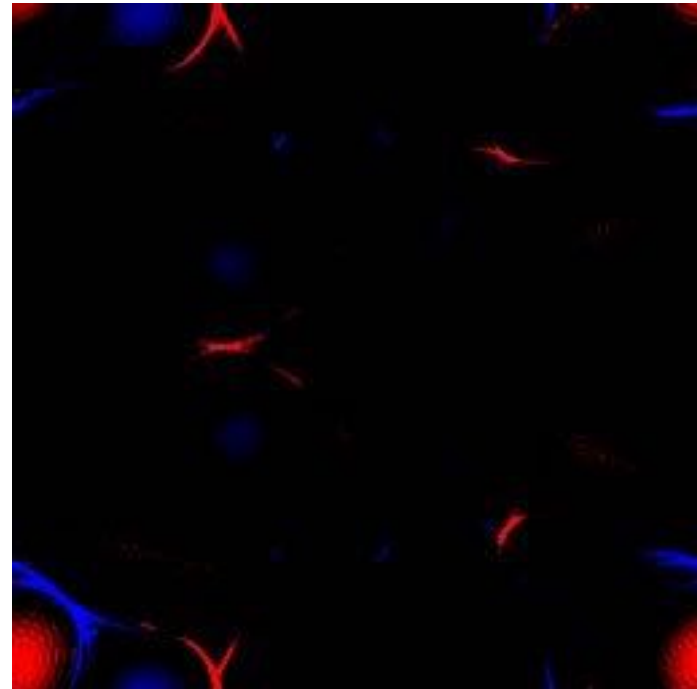


# Current sheets in RMHD

- ➡ Energy dissipation concentrates on very small structures known as current sheets, in which current density flows almost parallel to  $z$ .
- ➡ The picture shows **positive** and **negative** current density in a transverse cut at  $z = \frac{1}{2}$ , for pure RMHD (i.e.  $\varepsilon = 0$ ).
- ➡ When the Hall effect is considered, current sheets display the typical Petschek-like structure.

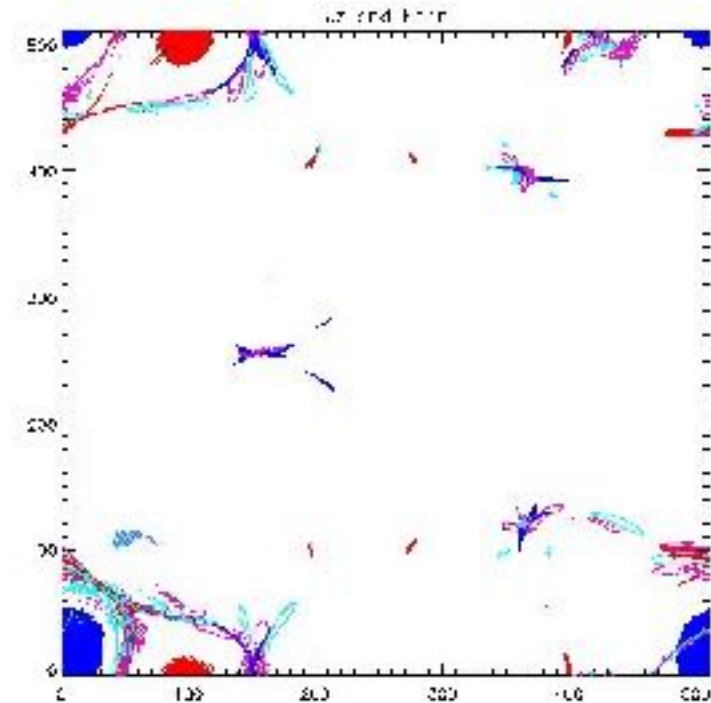
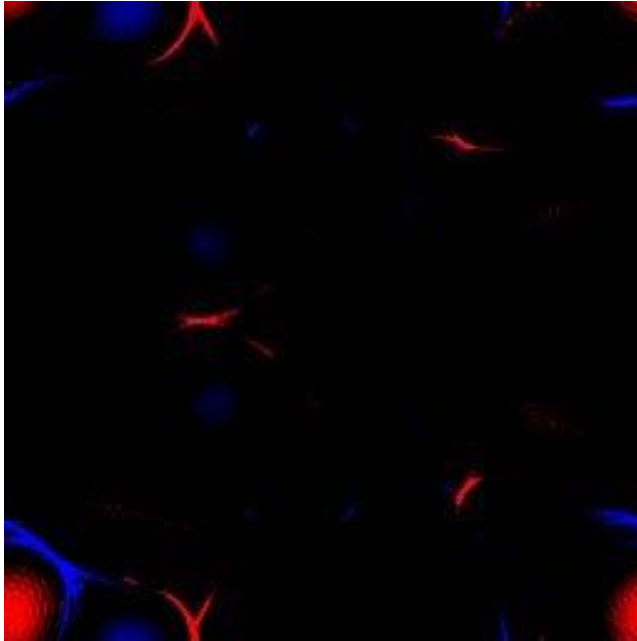


$\varepsilon = 0.0$



$\varepsilon = 0.1$

# Parallel electric field



➡ One of the important new features of the Hall effect, is the presence of a parallel electric field, i.e.  $E_{\parallel} = \frac{\vec{E} \cdot \vec{B}}{|\vec{B}|}$

➡ To order  $\alpha^2$  it can be computed as  $E_{\parallel} = \varepsilon (\partial_z b - [a, b])$

and of course it can potentially accelerate particles along magnetic field lines.

➡ Current density is displayed in **red** and **blue**, while contours coloured in **light blue** and **pink** correspond to the parallel electric field.

# Conclusions

- In this second lecture we introduced the two-fluid description as an extended version of MHD that goes beyond the ion and even the electron inertial lengths.
- Below the ion inertial length, we have the Hall-MHD approximation, which is an adequate theoretical framework to describe a number of astrophysical and laboratory applications.
- We also presented to so called reduced approximation, which is appropriate for plasmas embedded in relatively strong magnetic fields.
- We numerically integrated the Hall-MHD equations (spectral and Runge-Kutta) in the presence of a strong external magnetic field.
- As a first application, we showed RMHD simulations (no Hall effect yet) to study the internal dynamics of magnetic loops in the solar corona.
- We introduce the Hall effect and focused on its potential relevance in the dynamics of small scales and magnetic reconnection in the dissipative structures of turbulence.